

Cationic Borabenzene Complexes as Electron Accepting Groups for Molecular Material with Nonlinear Optical Properties

U. Behrens, T. Meyer-Friedrichsen, and J. Heck*

Hamburg, Institut für Anorganische und Angewandte Chemie der Universität

Received March 18th, 2003.

Dedicated to Professor Heinrich Nöth on the Occasion of his 75th Birthday

Abstract. The dinuclear dipolar borabenzene complexes $[(\eta^5\text{-C}_5\text{H}_5)\text{Fe}\{\mu\text{-}(\eta^5\text{-C}_5\text{H}_4)\text{C}_2(\eta^6\text{-BC}_5\text{H}_5)\}\text{ML}]_2\text{X}$ [ML = Ru($\eta^6\text{-C}_6\text{H}_6$), X = Cl (**4aCl**), PF₆ (**4aPF₆**), B(C₆H₅)₄ (**4aBPh₄**); ML = Rh($\eta^5\text{-C}_5\text{Me}_5$), X = Cl (**4bCl**), PF₆ (**4bPF₆**); ML = Ir($\eta^5\text{-C}_5\text{Me}_5$), X = Cl (**4cCl**), PF₆ (**4cPF₆**)] were synthesized by a nucleophilic substitution reaction of the trimethylphosphane adduct of borabenzene (**1**) with lithium ferrocenylacetylide, subsequent lithium-thallium exchange and coordination of the appropriate ML unit obtained from [Ru($\eta^6\text{-C}_6\text{H}_6$)Cl($\mu\text{-Cl}$)]₂, [M($\eta^5\text{-C}_5\text{Me}_5$)Cl($\mu\text{-Cl}$)]₂ (M = Rh, Ir); the formed chloride salts, which are soluble in water, were transformed to the PF₆ salts by adding [NH₄][PF₆] to the corresponding water solution. BPh₄ salts can be produced, when a methanolic solution of Na[BPh₄] were added to CH₂Cl₂-solutions of the appropriate

PF₆ salt. X-ray structure analyses of single crystals of **4aBPh₄** and **4bPF₆** were successful, illustrating the cation **4a⁺** in an ideal *cis*-conformation, whereas **4b⁺** displays a *cis*- and *trans*-conformation. Spectroscopic and cyclic voltammetry studies reveal a small but distinct donor-acceptor interaction between the ferrocenyl donor and the cationic borabenzene complex acceptor which increases in the order **4aPF₆** < **4cPF₆** < **4bPF₆**. The nonlinear optical properties of these donor-acceptor complexes were studied by means of hyper-Rayleigh scattering (HRS), resulting in the determination of small values for the first hyperpolarisability β , which increase in the same order as the donor-acceptor interaction.

Keywords: Dipolar dinuclear complexes; Nonlinear optical properties; Borabenzene complexes; Ferrocene; Hyper-Rayleigh scattering

Kationische Borabenzol-Komplexe als Elektronenakzeptor-Gruppen für molekulare Materialien mit nichtlinearoptischen Eigenschaften

Inhaltsübersicht. Der Weg zur Darstellung der zweikernigen, dipolaren Borabenzolkomplexe $[(\eta^5\text{-C}_5\text{H}_5)\text{Fe}\{\mu\text{-}(\eta^5\text{-C}_5\text{H}_4)\text{C}_2(\eta^6\text{-BC}_5\text{H}_5)\}\text{ML}]_2\text{X}$ [ML = Ru($\eta^6\text{-C}_6\text{H}_6$), X = Cl (**4aCl**), PF₆ (**4aPF₆**), B(C₆H₅)₄ (**4aBPh₄**); ML = Rh($\eta^5\text{-C}_5\text{Me}_5$), X = Cl (**4bCl**), PF₆ (**4bPF₆**); ML = Ir($\eta^5\text{-C}_5\text{Me}_5$), X = Cl (**4cCl**), PF₆ (**4cPF₆**)] führte über die nucleophile Substitutionsreaktion am Trimethylphosphanaddukt von Borabenzol (**1**) mit Lithiumferrocenylacetylid; das entstandene Lithiumsalz des ferrocenylethynylsubstituierten Borabenzols (**2**) wurde zunächst einer Li/Tl-Austauschreaktion unterworfen und zur Koordination an ML-Einheiten anschließend mit [Ru($\eta^6\text{-C}_6\text{H}_6$)Cl($\mu\text{-Cl}$)]₂, [M($\eta^5\text{-C}_5\text{Me}_5$)Cl($\mu\text{-Cl}$)]₂ (M = Rh, Ir) umgesetzt. Die entstandenen Cl-Salze sind wasserlöslich und lassen sich durch Zugabe von [NH₄][PF₆] zu wässrigen Lösungen der Chloride in die PF₆-Salze überführen. BPh₄-Salze können herge-

stellt werden, indem methanolische Lösungen von Na[BPh₄] zu CH₂Cl₂-Lösungen der entsprechenden PF₆-Salze gegeben werden. Einkristallstrukturanalysen von **4aBPh₄** und **4bPF₆** waren erfolgreich. Sie ergeben für das Kation **4a⁺** eine ideale *cis*-Konformation, während für **4b⁺** eine *cis*- und *trans*-Konformation gefunden wird. Spektroskopische und cyclovoltammetrische Studien zeigen eine geringe aber merkbare Donor-Akzeptor-Wechselwirkung zwischen dem Ferrocenyldonor und dem kationischen Borabenzolkomplex-Akzeptor, die in der Reihenfolge **4aPF₆** < **4cPF₆** < **4bPF₆** ansteigt. Die nichtlineare optischen Eigenschaften dieser Donor-Akzeptorkomplexe wurden mit Hilfe der hyper-Rayleigh-Streuungsmethode (HRS) untersucht. Danach konnten für die erste Hyperpolarisierbarkeit β relativ kleine Werte bestimmt werden, die in der gleichen Reihenfolge wie die Donor-Akzeptor-Wechselwirkung ansteigen.

Introduction

The concept of dipolar cationic heterobimetallic organometallic complexes for compounds with non-linear optical (NLO) properties [1] e.g. with high first order hyperpolaris-

ability β , has been shown to be very powerful [2]. These complexes consist of the combination of an organometallic electron donating and accepting group connected with a bridge, which enables electronic π -interaction between them. By far the most used donating units are sandwich type complexes, like ferrocene and ruthenocene, due to their inertness and facile synthetic manipulations [2c-t]. Another type of frequently used organometallic donating groups are half-sandwich complexes wherein the π -bridge is directly linked to the metal atom [2a, 2b].

For organometallic electron accepting groups carbonyl complexes were employed [2a, 2b, 2g, 2i, 2k, 2m, 2o.] as well as Fischer carbenes [2j] and cationic complexes of or-

* Prof. Dr. J. Heck
Institut für Anorgan. u. Angew. Chemie der Universität
Martin-Luther-King-Platz 6
D-20146 Hamburg
Tel.: +49 40 42838 6375
fax +49 40 42838 6945
email: juergen.heck@chemie.uni-hamburg.de

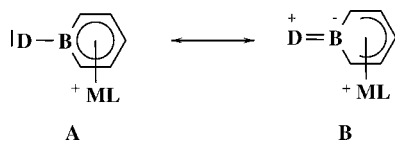


Figure 1 Mesomeric forms of cationic borabenzene complexes illustrating the electron accepting properties of the borabenzene entity.

ganic π -ligands [2d, 2e, 2j, 2n, 2p, 2r, 2t]. Recently, we have been able to demonstrate that the cationic η^6 -borabenzene complex of a cyclopentadienylcobalt unit can also be used as an electron accepting group for NLO chromophores [3]. Its electron accepting capability is reinforced by two effects: first by the cationic nature of the metal complex, and second, by the π -acidity of the boron atom (Figure 1). Additionally, the cationic borabenzene complexes are very stable in air [4], which would be an essential prerequisite for further applications.

In this paper we describe the synthesis, structure and spectroscopic properties of dipolar dinuclear borabenzene complexes wherein the electron donating group (ferrocenyl) and the accepting unit are separated by an ethynyl bridge.

Results and Discussion

Synthesis

Just recently, it was shown by *Fu* et al. [5] that boron-linked alkyne derivatives of boratabenzene can be obtained by nucleophilic substitution of the trimethylphosphane adduct of borabenzene (**1**) with lithium acetylides [6]. In order to combine a ferrocenyl donor with cationic borabenzene complexes the lithium salt of ferrocenylacetylide was successfully employed (Scheme 1, a). Since lithium salts of boratabenzene compounds as **2** display strong nucleophilicity, which hampers a good yield in the formation of borabenzene complexes of Ru, Rh and Ir, the lithium salt **2** was transformed to the thallium salt **3** by stirring **2** in acetonitrile in the presence of excess of thallium chloride (Scheme 1, b) [7].

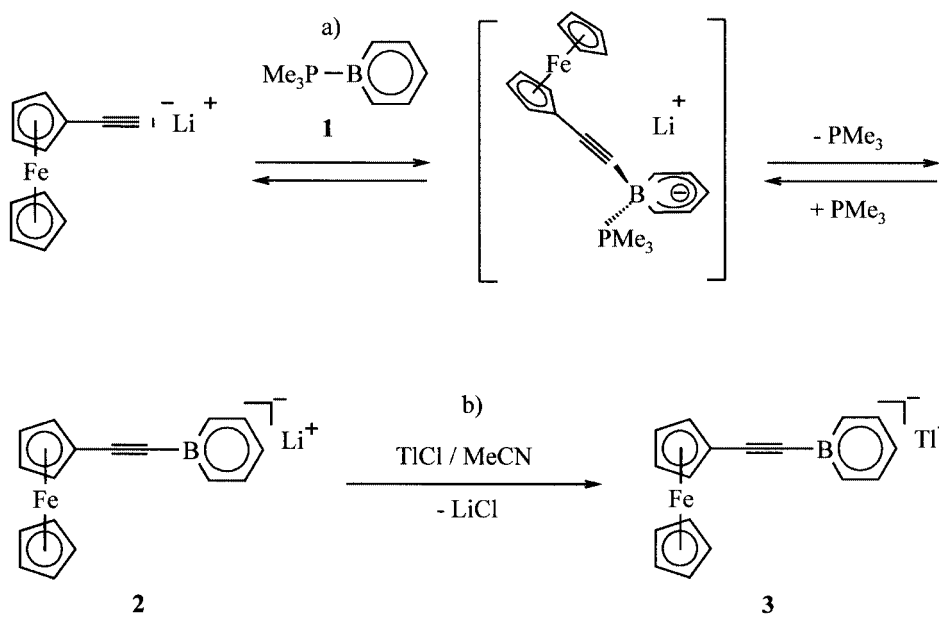
The thallium salt **3** was isolated once as a pyridine adduct and fully characterized. However, since the isolated yield of **3** is rather low (10 – 12%), the product of the metathesis reaction (Scheme 1, b) was allowed to react directly with the halfsandwich complexes $[\text{Ru}(\eta^6\text{-C}_6\text{H}_6)\text{Cl}_2]_2$, $[\text{Rh}(\eta^5\text{-C}_5\text{Me}_5)\text{Cl}_2]_2$ and $[\text{Ir}(\eta^5\text{-C}_5\text{Me}_5)\text{Cl}_2]_2$ without further isolation of the thallium salt **3** (Scheme 2). The intermediate generated chloride salts **4aCl**, **4bCl** and **4cCl** are water soluble and can be precipitated as PF_6^- salts by adding $[\text{NH}_4][\text{PF}_6]$. The tetraphenyl borate salt **4aBPh₄** was obtained by adding a methanol solution of $\text{Na}[\text{BPh}_4]$ to a solution of **4aPF₆** in CH_2Cl_2 . Crystals of **4a BPh₄** are stable in air for years and corresponding solutions for weeks at least.

Solid state structure

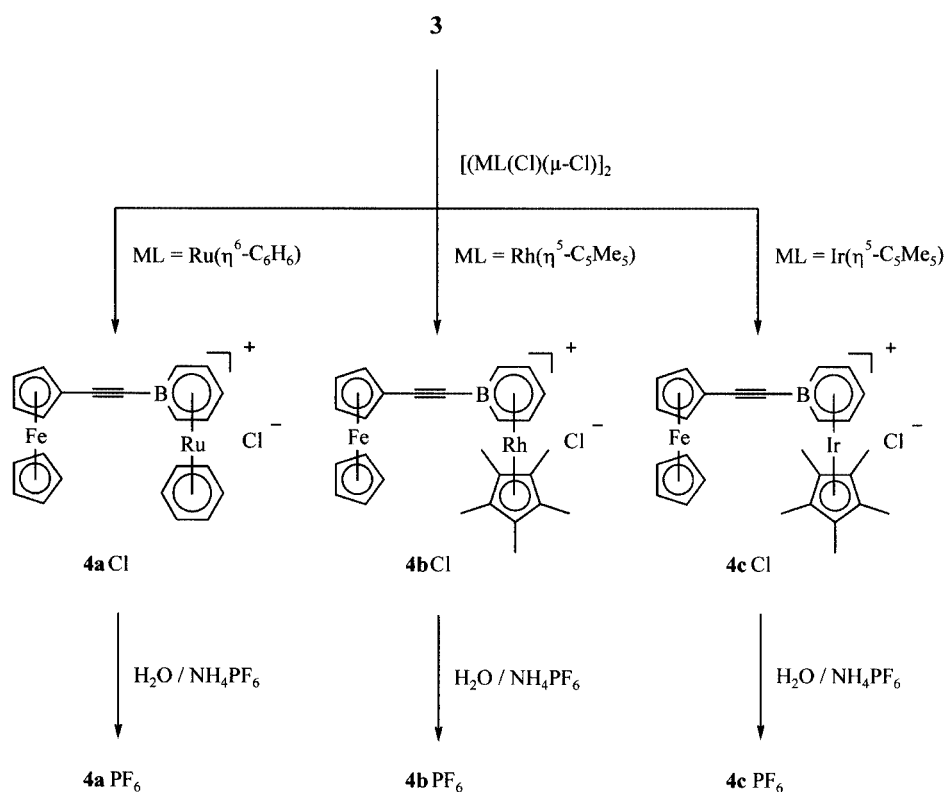
The PF_6^- -salts of **4a**, **4b** and **4c** crystallize in very thin plates, which were not very proper for X-ray structure analyses. Therefore, **4aPF₆** was transformed to the BPh_4^- -salt and suitable crystals were obtained by gasphase diffusion of Et_2O into a concentrated solution of **4aBPh₄** in acetonitrile. **4aBPh₄** crystallizes in the triclinic space group $P\bar{1}$ with two independent molecules in the asymmetric unit. The cationic bis(sandwich)complex **4a⁺** adopts an almost perfect *cis*-conformation (Figure 2); the substituted Cp ligand of the ferrocenyl unit is twisted only about $1.9(2)^\circ$ with respect to the borabenzene ligand. The two Cp ligands of the ferrocenyl moiety are in an eclipsed conformation, whereas a *gauche* conformation is found for the two six-membered rings of the borabenzene complex. The iron atom is placed equidistant with respect to the planes of the two Cp ligands (165.2(2) pm and 165.1(2) pm, respectively), and the Fe–C bond lengths are quite normal for monosubstituted ferrocene derivatives with weak electronic interaction with the substituent.

The borabenzene complex moiety reveals the typical structural features found for similar-sandwich complexes: the Ru–C(*benzene*) distances are as expected (216.9(4) – 220.9(4) pm), however, a strong variation of the C,C bond distances is found, indicating some disorder of the benzene ligand. The Ru–C(*borabenzene*) bond lengths fall in the range of 218.8(4) – 224.2(4) pm (Table 2), with the shortest Ru–C bond lengths in *p*-position with respect to the boron atom, which is in agreement with other borabenzene complexes [8]. The Ru–B bond length of 237.8(5) pm corresponds to published metal-boron distances found for other borabenzene complexes [9].

The four atoms C1, C11, C12, and B1, forming the bridge between the donor and the acceptor, are arranged in an almost linear fashion (C1–C11–C12: $178.6(4)^\circ$, C11–C12–B1: $175.2(4)^\circ$). Of particular interest for donor-acceptor molecules is the bond length variation in the π -linker, since it manifests the extent of electronic communication between the donor and the acceptor, and gives some hints on NLO-properties [10,11]. However, complex cation **4a⁺** contains a C≡C-length about 120.3(5) pm, which is slightly elongated compared to 118.3 pm in R–C≡C–R with isolated carbon-carbon triple bonds or in the donor-acceptor compound 4-nitro-4'-amino tolane [11]. Whether this small elongation is caused by a delocalisation of the π -bonding electrons, as depicted in Figure 3, is not quite clear, since the carbon-carbon and carbon-boron single bonds (143.3(5) and 155.0(6) pm, respectively) of the acetylenic linker in **4a⁺** are as long as the corresponding bond lengths for the donor-acceptor tolane compound [11] and diborylacetylenes [12], respectively. Therefore, a pronounced donor-acceptor interaction in **4a⁺**, which may be deduced from structural features of the π -bridge between the donor and the acceptor, cannot be concluded. This is in good harmony with results obtained from theoretical calculation about ethynylboranes which prove a very small tendency to form delocalized heteroallenes (Figure 4) [13].



Scheme 1 Synthesis of the thallium salt of ferrocenylethynyl boratabenzene (**3**)



Scheme 2 Synthesis of $[(\eta^5\text{-C}_5\text{H}_5)\text{Fe}\{\mu\text{-}(\eta^5\text{-C}_5\text{H}_4)\text{C}_2(\eta^6\text{-BC}_5\text{H}_5)\}\text{ML}]\text{X}$, $\text{X} = \text{Cl}, \text{PF}_6$

Crystals of **4bPF₆** were obtained by diffusion of an Et₂O layer into a concentrated solution of **4bPF₆** in CH₂Cl₂. A red, plate-shaped crystal was subjected to X-ray crystal structure determination. For compound **4bPF₆** a large B-centred cell with an orthorhombic metric was found (see table 1, cell parameters). However, there is no mmm sym-

metry in the intensity data set, but only monoclinic symmetry with the b axis (1057.48 pm) as the monoclinic axis. In a monoclinic setting (half volume of the orthorhombic cell; half ac diagonal as c axis) the space group is P2₁/c. For convenience the orthorhombic cell setting was maintained (non standard space group B2₁/d). In the structure of **4bPF₆**

Table 1 Crystallographic data of $[(\eta^5\text{-C}_5\text{H}_5)\text{Fe}\{\mu\text{-}(\eta^5\text{-C}_5\text{H}_4)\text{C}_2(\eta^6\text{-BC}_5\text{H}_5)\}\text{Ru}(\eta^6\text{-C}_6\text{H}_6)]\text{[B}(\text{C}_6\text{H}_5)_4\text{]} (4\mathbf{aBPPh}_4)$ and $[(\eta^5\text{-C}_5\text{H}_5)\text{Fe}\{\mu\text{-}(\eta^5\text{-C}_5\text{H}_4)\text{C}_2(\eta^6\text{-BC}_5\text{H}_5)\}\text{Rh}(\eta^5\text{-C}_5\text{Me}_5)]\text{PF}_6 (4\mathbf{bPF}_6)$

| | 4aBPPh ₄ | 4bPF ₆ |
|--|--|---|
| Empirical formula | C ₄₇ H ₄₀ B ₂ FeRu | C ₂₇ H ₂₉ BF ₆ FePRh |
| Formula mass | 783.33 | 668.04 |
| <i>T</i> /K | 293 | 153 |
| λ /pm | 71.073 | 71.073 |
| Crystal size /mm ³ | 0.4 x 0.4 x 0.2 | 0.2 x 0.2 x 0.05 |
| Crystal system | triclinic | monoclinic |
| Space group | P $\bar{1}$ | B2 ₁ /d |
| <i>a</i> /pm | 1057.0(2) | 692.27(5) |
| <i>b</i> /pm | 1092.2(2) | 1057.48(8) |
| <i>c</i> /pm | 1835.3(4) | 7083.4(5) |
| α /° | 86.73(3) | 90 |
| β /° | 75.18(3) | 90.00 |
| γ /° | 61.34(3) | 90 |
| <i>V</i> /10 ⁶ pm ³ | 1791.9(6) | 5185.5(7) |
| <i>Z</i> | 2 | 8 |
| ρ_{calc} /Mg/m ³ | 1.452 | 1.711 |
| μ /mm ⁻¹ | 0.860 | 1.32 |
| $2\sigma_{\text{max}}$ /° | 50 | 54 |
| Index range | -11 ≤ <i>h</i> ≤ 0 -12 ≤ <i>k</i> ≤ 11 -21 ≤ <i>l</i> ≤ 21 | -8 ≤ <i>h</i> ≤ 8 -13 ≤ <i>k</i> ≤ 13 -89 ≤ <i>l</i> ≤ 89 |
| Reflections total/indep. | 6802/6218 | 30541/5803 |
| Reflections [<i>I</i> >4σ(<i>I</i>)] | 5392 | 3734 |
| Parameters | 460 | 350 |
| GoF ^{a)} | 1.023 | |
| <i>R</i> factor [<i>I</i> >4σ(<i>I</i>) ^{b)} | 0.038 | 0.069 |
| <i>wR</i> 2 (all data) ^{b)} | 0.100 | 0.157 |
| Resd. min/max (e/Å ⁻³) | -0.98/1.25 | -2.08/1.11 |

$$^a) \text{ GoF (goodness of fit)} = \sqrt{\frac{\sum w(F_o^2 - F_c^2)^2}{n-p}}$$

(*n* = numbers of reflections, *p* = numbers of parameters).

$$^b) R1 = \frac{\sum ||F_o| - |F_c||}{\sum |F_o|}; wR2 = \sqrt{\frac{\sum w(F_o^2 - F_c^2)^2}{\sum w(F_o^2)^2}}$$

the Rh atom is disordered over two sites (s.o.f. 0.5/0.5). Refinement as a twin (twin components 0.8 and 0.2) lowered the conventional *R* value from about 0.11 to 0.069.

Remarkably, the molecular structure of **4b**⁺ is represented by an ideal *cis*- and *trans*-conformation in the crystalline state (Figure 5). Usually, sandwich-type donor-acceptor pairs seem to prefer a *cis*-conformation, when they are separated at least by a C₂-linker like ethendiyl or ethyn-diyl [2d, 2j, 2n, 2t]. One exception is known for a dinuclear monohydro sesquifulvalene which bears a pentamethylated cyclopentadienyl (Cp*) ligand as well [2t]. Apparently, the steric interaction between the Cp* ligand of one sandwich unit and the Cp ligand of the other one does not prefer the *cis*-arrangement of both sandwich moieties as the only conformer.

As already observed for the Ru derivative **4a**⁺, the Cp ligand and the joined borabenzene ligand deviate only about 4.4° from coplanarity and the linking unit C1, C11, C12, and B(1) is linear arranged (C1-C11-C12: 177.9°; C11-C12-B1: 177.5°). The bond lengths within the π-linker are very similar to the corresponding bond lengths of **4a**⁺, only the C12-B1 distance (151.6(9) pm) seems to be slightly shortened with respect to C12-B1 of **4a**⁺ (155.0(6) pm).

Table 2 Selected interatomic distances /pm and angles /° of $[(\eta^5\text{-C}_5\text{H}_5)\text{Fe}\{\mu\text{-}(\eta^5\text{-C}_5\text{H}_4)\text{C}_2(\eta^6\text{-BC}_5\text{H}_5)\}\text{Ru}(\eta^6\text{-C}_6\text{H}_6)]\text{[B}(\text{C}_6\text{H}_5)_4\text{]} (4\mathbf{aBPPh}_4)$ and $[(\eta^5\text{-C}_5\text{H}_5)\text{Fe}\{\mu\text{-}(\eta^5\text{-C}_5\text{H}_4)\text{C}_2(\eta^6\text{-BC}_5\text{H}_5)\}\text{Rh}(\eta^5\text{-C}_5\text{Me}_5)]\text{PF}_6 (4\mathbf{bPF}_6)$

| | 4aBPPh ₄ | 4bPF ₆ |
|-----------------------------------|---------------------|--|
| C1 – C2 | 143.3(5) | 140.9(9) |
| C2 – C3 | 141.4(5) | 137.2(10) |
| C3 – C4 | 141.4(5) | 140.5(11) |
| C4 – C5 | 141.2(5) | 143.9(10) |
| C5 – C1 | 144.2(5) | 145.0(9) |
| C6 – C7 | 142.8(6) | 140.2(10) |
| C7 – C8 | 141.0(6) | 148.0(11) |
| C8 – C9 | 141.8(6) | 139.9(12) |
| C9 – C10 | 142.2(6) | 137.4(10) |
| C10 – C6 | 140.5(6) | 141.4(10) |
| C1 – C11 | 143.3(5) | 143.2(8) |
| C11 – C12 | 120.3(5) | 122.0(8) |
| C12 – B1 | 155.0(6) | 151.6(9) |
| C13 – B1 | 153.1(7) | 153.6(10) |
| C13 – C14 | 140.9(6) | 137.9(8) |
| C14 – C15 | 140.9(7) | 141.2(8) |
| C15 – C16 | 140.8(7) | 140.4(9) |
| C16 – C17 | 141.1(6) | 141.7(9) |
| C17 – B1 | 150.7(8) | 152.5(9) |
| Fe – C1 | 204.3(4) | 203.5(8) |
| Fe – C2 | 204.5(3) | 203.1(9) |
| Fe – C3 | 205.0(3) | 204.5(9) |
| Fe – C4 | 205.5(4) | 202.0(9) |
| Fe – C5 | 204.4(4) | 206.4(9) |
| Fe – [C1-C5] ^{a)} | 165.1(2) | 164.6(5) |
| Fe – [C6-C10] ^{b)} | 165.2(2) | 165.8(5) |
| M – B1 | 237.7(4) | M = Rh1 229.7(9) Rh2 228.7(8) |
| M – C13 | 223.9(4) | Rh1 227.3(7) Rh2 228.2(7) |
| M – C14 | 220.3(4) | Rh1 219.9(7) Rh2 222.2(7) |
| M – C15 | 218.8(4) | Rh1 205.6(8) Rh2 211.9(8) |
| M – C16 | 220.1(4) | Rh1 205.5(8) Rh2 208.6(9) |
| M – C17 | 224.2(4) | Rh1 213.7(8) Rh2 211.0(8) |
| M – [B1-C17] ^{c)} | 171.3(2) | Rh1 161.2(5) Rh2 163.3(5) |
| Ru – [C18-C23] ^{d)} | 169.7(2) | Rh1 182.7(5) |
| Rh – [C18-C23] ^{e)} | | Rh2 185.1(5) |
| C1 – C11 – C12 | 178.6(4) | 177.9(8) |
| C11 – C12 – B1 | 175.2(4) | 177.5(8) |
| [C1 – C5][B1 – C17] ^{f)} | 1.9(2)° | 4.3(5)° |

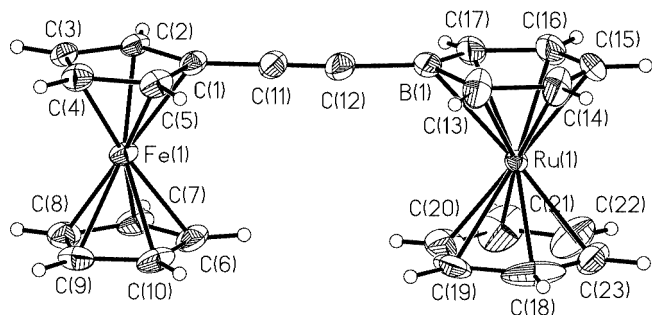
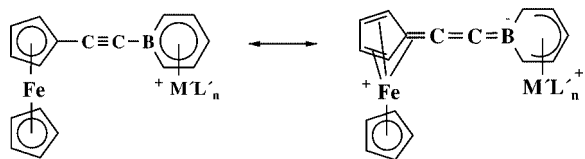
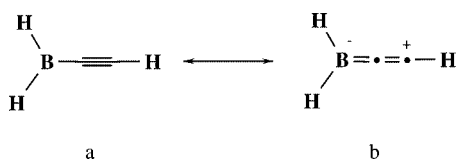
^{a)} [C1-C5]: best plane of C1, C2, C3, C4 and C5; ^{b)} [C6-C10]: best plane of C6, C7, C8, C9 and C10; ^{c)} [B1-C17]: best plane of B1, C13, C14, C15, C16 and C17; ^{d)} [C18-C23]: best plane of C18, C19, C20, C21, C22 and C23; ^{e)} [C18-C22]: best plane of C18, C19, C20, C21 and C22; ^{f)} inter planar angle between [C1-C5] and [B1-C17].

The coordination of the Rh atom to the borabenzene ligand demonstrates the typical bonding mode with a long rhodium-boron distance (229.7(9) and 228.7(8) pm) similar to other Rh-B distances in comparable borabenzene complexes, and a general Rh-C(*borabenzene*) bond shortening in the opposite position. This bonding situation very much resembles the common coordination feature of borabenzene complexes (vide supra) [9,14], however, in this case a more precise statement suffers from the disorder of **4bPF**₆. The

Table 3 Selected spectroscopic data of the bimetallic borabenzene complexes $[(\eta^5\text{-C}_5\text{H}_5)\text{Fe}\{\mu\text{-}(\eta^5\text{-C}_5\text{H}_4)\text{C}_2(\eta^6\text{-BC}_5\text{H}_5)\}\text{ML}]\text{PF}_6$ [$\text{ML} = \text{Ru}(\eta^6\text{-C}_6\text{H}_6)$ (**4a**PF₆), $\text{Rh}(\eta^5\text{-C}_5\text{Me}_5)$ (**4b**PF₆), $\text{Ir}(\eta^5\text{-C}_5\text{Me}_5)$ (**4c**PF₆)]

| ML | ¹ H NMR ^{a)} δ/ppm | | | | | | IR ^{c)} ν _{C=C} cm ⁻¹ | Electrochemistry | | UV-VIS | | HRS β ⁱ⁾ | |
|--|---|-------------------------------|-------------------|---------------------|---------------------|------|--|------------------------------------|------------------------------------|---|--|------------------------|------------------------------------|
| | C ₅ H ₄ | C ₅ H ₅ | H-4 ^{b)} | H-3,5 ^{b)} | H-2,6 ^{b)} | L | | E _{1/2(ox)} ^{d)} | E _{pc(red)} ^{e)} | λ _{max} ^{d)} (ε) ^{g)} CH ₂ Cl ₂ | λ _{max} ^{d)} (ε) ^{g)} MeCN | | Δν ^{h)} /cm ⁻¹ |
| Ru(η ⁶ -C ₆ H ₆) (4a) | 4.32, 4.50 | 4.25 | 5.39 | 6.39 | 6.39 | 6.60 | 2166 (m) | 0.10 | -1.84 | 288(11120) | 288(8080) | - | n.d. |
| Rh(η ⁵ -C ₅ Me ₅) (4b) | 4.33, 4.55 | 4.28 | 5.62 | 6.68 | 6.52 | 2.26 | 2156 (m) | 0.18 | -1.6 | 446 (970) 293(12200) | 440 (600) 290(12480) | -305 -306 | 59 |
| Ir(η ⁵ -C ₅ Me ₅) (4c) | 4.31, 4.52 | 4.26 | 5.64 | 6.65 | 6.65 | 2.36 | 2160 (m) | 0.13 | -2.05 | 335 (7070) 456 (1330) 292(18860) | 331 (5810) 450 (sh) 288(12780) | -361 - -476 | 46 |
| | | | | | | | | | | ≈360 (sh) 442(985) | ≈350 (sh) 442(480) | - - | |

^{a)} 200 MHz, [D₆]acetone, room temperature; δ (FcH) = 4.15 ppm; ^{b)} borabenzene ligand; ^{c)} KBr pellets; ^{d)} half-wave potential for oxidation in V vs. [FcH]/[FcH]⁺; ^{e)} E_{pc} = peak potential in V vs [FcH]/[FcH]⁺, ν = 50 mV/s; ^{f)} nm; ^{g)} M⁻¹cm⁻¹; ^{h)} Δν = ν(CH₂Cl₂) - ν(MeCN), ⁱ⁾ given as units of 10⁻³⁰ esu; as reference *p*-nitroaniline was used: β(MeNO₂) = 34.6 mol 10⁻³⁰ esu [28].

**Figure 2** Molecular structure of $[(\eta^5\text{-C}_5\text{H}_5)\text{Fe}\{\mu\text{-}(\eta^5\text{-C}_5\text{H}_4)\text{C}_2(\eta^6\text{-BC}_5\text{H}_5)\}\text{Ru}(\eta^6\text{-C}_6\text{H}_6)]\text{[B}(\text{C}_6\text{H}_5)_4\text{]} (\mathbf{4aBPPh}_4)$ in the crystalline state (50% ellipsoids, the counterion $[\text{BPh}_4]^-$ is omitted for clarity)**Figure 3** Limiting mesomeric forms of the cationic borabenzene complex $[(\eta^5\text{-C}_5\text{H}_5)\text{Fe}\{\mu\text{-}(\eta^5\text{-C}_5\text{H}_4)\text{C}_2(\eta^6\text{-BC}_5\text{H}_5)\}\text{ML}]^+$ [$\text{ML} = \text{Ru}(\eta^6\text{-C}_6\text{H}_6)$, $\text{Rh}(\eta^5\text{-C}_5\text{Me}_5)$, $\text{Ir}(\eta^5\text{-C}_5\text{Me}_5)$]**Figure 4** Limiting mesomeric forms for ethynyl boranes

mean values of other bond lengths are as expected as well taking into account the disorder which results in quite dif-

ferent values for comparable bonds e.g. within the Cp ligands.

Spectroscopic Properties

The assignment of the ¹H and ¹³C NMR signals was performed by using the splitting pattern in the ¹H NMR spectra and by means of ¹H¹³C correlation spectroscopy. From the ¹H NMR spectroscopic data (Table 3) it becomes evident that the shifts of the resonance signals can be separated into two domains: one for the borabenzene ligand (5.39 – 6.68 ppm) and the other for the ferrocenyl donor (4.25 – 4.55 ppm). The general low field shifts of the ferrocenyl signals compared to the unsubstituted ferrocene (δ = 4.15) indicate the electron accepting capability of the cationic borabenzene complex moiety. From the relative low-field shift of the Cp signals of the ferrocene donor an electron withdrawing strength can be deduced in the order $\text{Ru}(\eta^6\text{-C}_6\text{H}_6) < \text{Ir}(\eta^5\text{-C}_5\text{Me}_5) < \text{Rh}(\eta^5\text{-C}_5\text{Me}_5)$, although the differences are not very pronounced.

This order would be in agreement with the position of the stretching mode of the carbon-carbon triple bond in the IR spectra of **4a**PF₆, **4b**PF₆ and **4c**PF₆, if only electronic changes in the acetylenic bridge are important (Table 3): with increasing contribution of the cummulenic resonance form a decrease in the bond order of the central carbon-carbon bond is expected (Figure 3), which causes a decrease in the energy of the corresponding carbon-carbon stretching vibration. However, the differences in the C≡C-stretching energies are very small and have to be regarded with care, since they may additionally be influenced by mechanical coupling effects, which, in particular, are important for linear arranged atoms.

The cyclic voltammetry (CV) study of the complexes **4a**PF₆, **4b**PF₆ and **4c**PF₆ reveal an electrochemically reversible oxidation step, the potential and characteristic of which are indicative for the ferrocenyl entity. Therefore, this

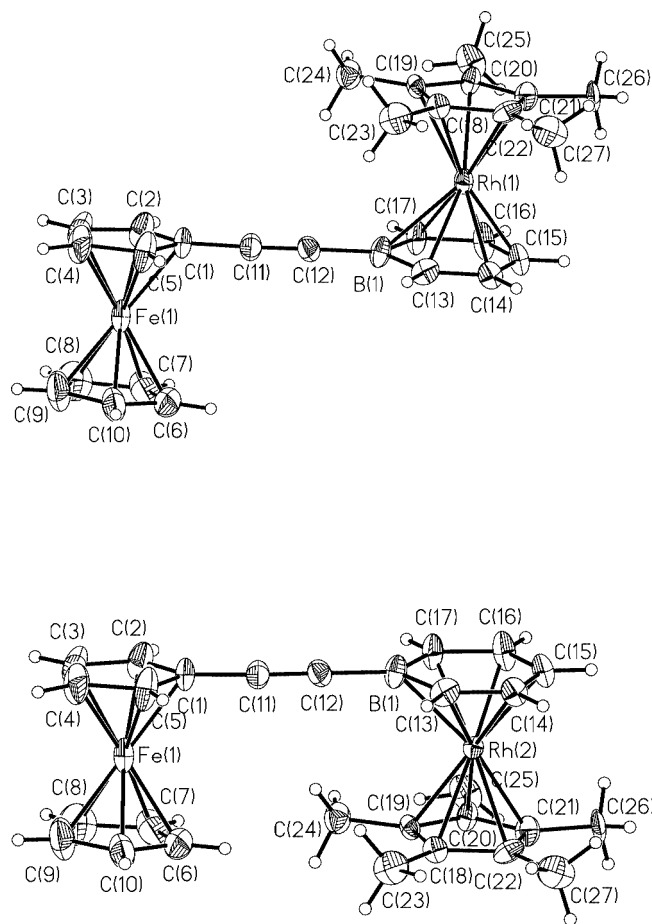


Figure 5 Molecular structure of $[(\eta^5\text{-C}_5\text{H}_5)\text{Fe}\{\mu\text{-}(\eta^5\text{-C}_5\text{H}_4)\text{C}_2(\eta^6\text{-BC}_5\text{H}_5)\}\text{Rh}(\eta^5\text{-C}_5\text{Me}_5)]\text{PF}_6$ (**4bPF**₆) in the crystalline state (50% ellipsoids, the counterion $[\text{PF}_6]^-$ is omitted for clarity). This figure includes both conformers which gives rise for a disorder (top: *trans*-conformer, bottom: *cis*-conformer) (For more details see text)

oxidation step is combined with a one-electron transfer (Table 3). In addition, an irreversible reduction wave can be recorded at very low potential (< -1.60 V vs $[\text{FcH}]/[\text{FcH}]^+$) which is attributed to the borabenzene complex unit (Figure 6). A comparison of the peak currents of the two redox steps proves a one-electron transfer for the reduction as well. Whereas for **4aPF**₆ and **4cPF**₆ this reduction step is completely irreversible, for **4bPF**₆ a partial electrochemical reversibility is observed (Figure 6). In addition a small re-oxidation wave appears at about 1 V anodically shifted with respect to the reduction step. This wave is only observed, when the reduction step was first recorded; in contrast to it, starting at -1.0 V vs. $[\text{FcH}]/[\text{FcH}]^+$ and recording the CV first anodically, no corresponding wave is observed. This result indicates that the oxidation wave at about -0.6 V is a consequence of a chemical reaction upon the reduction at -1.6 V vs. FcH/FcH^+ [15].

The clear anodic shift of the reversible oxidation potential $E_{1/2}(\text{ox})$ in relation to unsubstituted ferrocene is due to the electron accepting capability of the cationic boraben-

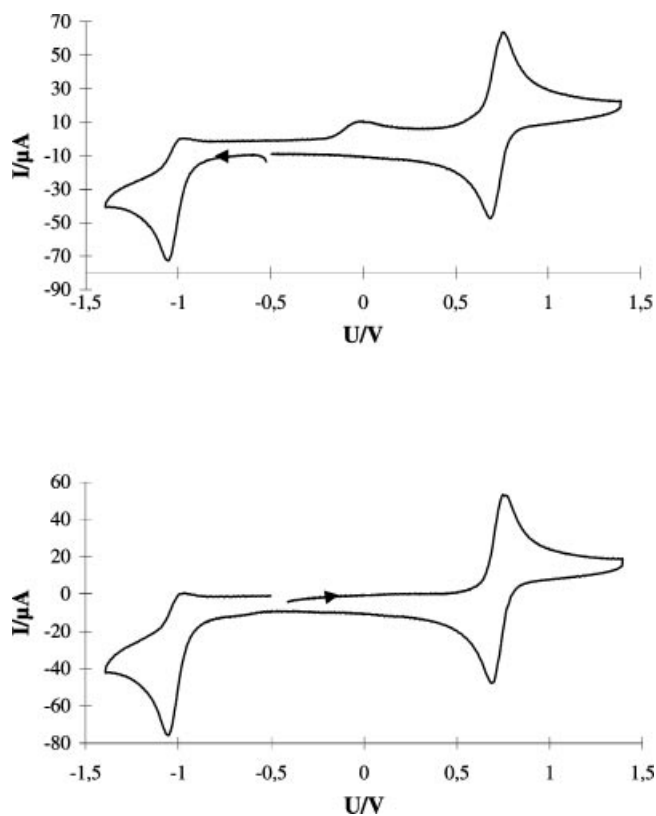


Figure 6 Representative cyclic voltammogram for $[(\eta^5\text{-C}_5\text{H}_5)\text{Fe}\{\mu\text{-}(\eta^5\text{-C}_5\text{H}_4)\text{C}_2(\eta^6\text{-BC}_5\text{H}_5)\}\text{ML}]\text{PF}_6$ [$\text{ML} = \text{Ru}(\eta^6\text{-C}_6\text{H}_6)$; $\text{Rh}(\eta^5\text{-C}_5\text{Me}_5)$; $\text{Ir}(\eta^5\text{-C}_5\text{Me}_5)$]; here $\text{ML} = \text{Rh}(\eta^5\text{-C}_5\text{Me}_5)$ (**4bPF**₆). Upper CV: scan direction is cathodic first, then anodic; lower CV: scan direction is first anodic, then cathodic (the voltage is measured against Ag/AgCl).

zene substituent. However, the extent of the anodic shift of $E_{1/2}(\text{ox})$ for **4aPF**₆ - **4cPF**₆ is distinctly lower than for the sesquifulvalene congener $[(\eta^5\text{-C}_5\text{H}_5)\text{Fe}\{\mu\text{-}(\eta^5\text{-C}_5\text{H}_4)\text{C}_2(\eta^7\text{-C}_7\text{H}_6)\}\text{Cr}(\text{CO})_3]^+$ [2d] with $E_{1/2}(\text{ox}) = 220$ mV vs. $[\text{FcH}]/[\text{FcH}]^+$. It is worthwhile to note that the increasing electron withdrawing capability of the metal-ligand unit ML on the oxidation potential $E_{1/2}$ reflects the same order as found from the NMR and IR studies.

UV-vis spectroscopic studies were performed with solutions of different polarity such as dichloromethane and acetonitril, to elucidate solvatochromism which gives an indication of the dipole change $\Delta\mu$ between the ground and the excited state [16], and is thus relevant for the first hyperpolarisability β . The UV-vis spectra of **4aPF**₆ - **4cPF**₆ obtained from CH_2Cl_2 and MeCN, illustrate three absorption maxima of quite different intensities (Figure 7, Table 3). The strongest absorption maximum is observed at $\lambda < 300$ nm, which undergoes no (for **4aPF**₆) or moderate hypsochromic shift, when the solvent has changed from CH_2Cl_2 to MeCN (Figure 8). The absorption maximum between 300 and 400 nm, which is much lower in intensity, is only resolved for the rhodium complex **4bPF**₆, whereas for

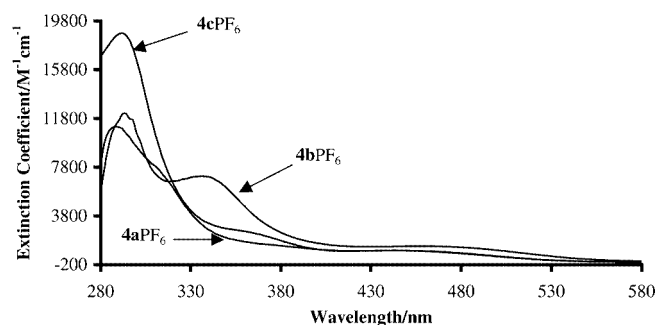


Figure 7 UV-vis spectra of $[(\eta^5\text{-C}_5\text{H}_5)\text{Fe}\{\mu\text{-}(\eta^5\text{-C}_5\text{H}_4)\text{C}_2(\eta^6\text{-BC}_5\text{H}_5)\}\text{ML}]\text{PF}_6$ [ML = Ru($\eta^6\text{-C}_6\text{H}_6$) (**4aPF**₆), Rh($\eta^5\text{-C}_5\text{Me}_5$) (**4bPF**₆), Ir($\eta^5\text{-C}_5\text{Me}_5$) (**4cPF**₆)] obtained from CH₂Cl₂ solutions.

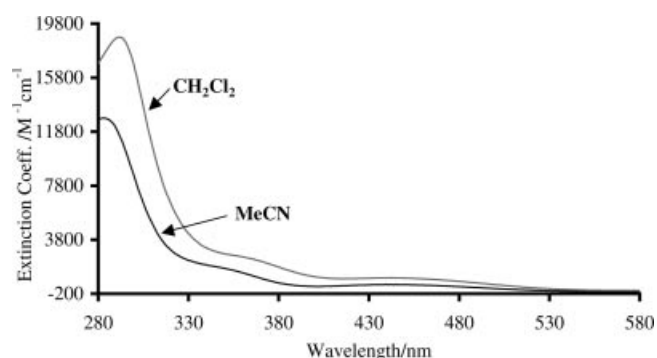


Figure 8 UV-vis spectra of $[(\eta^5\text{-C}_5\text{H}_5)\text{Fe}\{\mu\text{-}(\eta^5\text{-C}_5\text{H}_4)\text{C}_2(\eta^5\text{-BC}_5\text{H}_5)\}\text{Ir}(\eta^6\text{-C}_5\text{Me}_5)]\text{PF}_6$ (**4cPF**₆) obtained from CH₂Cl₂ and MeCN solutions illustrating the solvatochromic effect.

4aPF₆ and **4cPF**₆ only a shoulder is observed, which hampers the determination of the solvatochromic effect.

A weak absorption maximum ($\epsilon < 1000 \text{ M}^{-1}\text{cm}^{-1}$) is recorded beyond 400 nm. Since this absorption band is only poorly resolved, no solvatochromism is estimated for this energetically low lying weak absorption band.

In general a negative solvatochromism of the absorption bands in the electronic excitation spectra for **4aPF**₆, **4bPF**₆, and **4cPF**₆ is observed, which is characteristic for other cationic donor-acceptor complexes, and indicate a donor-acceptor charge-transfer transition upon electronic excitation. However, the extent of the hypsochromic shift is only moderate compared to corresponding cationic sesquifulvalene type complexes giving raise for a poor polarisability, and thus also poor hyperpolarisability.

NLO Measurements

The cationic nature of the borabenzene complexes **4a**⁺–**4c**⁺ requires the hyper-Rayleigh scattering (HRS) [17] as the only method to determine the first hyperpolarisability β which presents the molecular capability to double the frequency of incoming light. However, a pit-fall of the HRS method may be fluorescence due to two-photon ab-

sorption [18]. Amongst different methods [18], we chose for the “low-cost” check for the two photon-absorption induced fluorescence (TFP), which was recently described [2s, 19], and used bandpass filters with peak transmittance at different wavelengths, which are introduced in front of the photomultiplier of the HRS set-up. The broad fluorescence signal, which yields the emission maximum at $\lambda/2$ of the fundamental wavelength only by chance, is easily discerned from the narrow second harmonic signal at $\lambda/2$. In course of this study no fluorescence intensity was observed.

The NLO studies on **4aPF**₆ – **4cPF**₆ have been performed in nitromethane solutions with concentrations at about 10^{-4} – 10^{-6} M. For complex **4aPF**₆ no second harmonic generation (SHG) could be observed in contrast to **4bPF**₆ and **4cPF**₆ (Table 3) [20]. The experimentally obtained first hyperpolarisabilities β for **4bPF**₆ and **4cPF**₆ are still rather low and considerably smaller than β values obtained from similar ferrocene containing NLO chromophores. The corresponding static first hyperpolarisability was not calculated, since all of the charge-transfer transitions may contribute to the SHG effect. Nevertheless, the characteristic of the electronic excitation spectra of all compounds under investigation is quite similar, hence the contribution to the resonance enhancement of β will be similar for **4aPF**₆, **4bPF**₆ and **4cPF**₆. Therefore, a conservative comparison of the SHG effect of the borabenzene cations may be allowed, which demonstrates a slight increase of the β values in the order **4aPF**₆ < **4cPF**₆ < **4bPF**₆. This order matches the extent of the donor-acceptor interaction demonstrated by ¹H NMR, IR and cyclic voltammetry data (*vide supra*).

Conclusions

Three different dinuclear, cationic borabenzene complexes $[(\eta^5\text{-C}_5\text{H}_5)\text{Fe}\{\mu\text{-}(\eta^5\text{-C}_5\text{H}_4)\text{C}_2(\eta^6\text{-BC}_5\text{H}_5)\}\text{ML}]^+$ [(ML = Ru($\eta^6\text{-C}_6\text{H}_6$) (**4a**⁺), Rh($\eta^5\text{-C}_5\text{Me}_5$) (**4b**⁺), Ir($\eta^5\text{-C}_5\text{Me}_5$) (**4c**⁺)] displaying donor-acceptor interactions, have been successfully synthesized and fully characterised: X-ray structure determinations of complex **4aBPh**₄ and **4bPF**₆ reveal an almost unchanged acetylenic linker between the ferrocene donor and the cationic borabenzene complex moiety compared to more or less symmetrically substituted alkynes. However, a weak donor-acceptor interaction, which may be considered as a subtle contribution of the cummulenic resonance form to the ground state (Figure 3), can be concluded from ¹H NMR, IR and cyclic voltammetry data. NLO studies on **4aPF**₆, **4bPF**₆ and **4cPF**₆ by means of HRS experiments point to a slight increasing first hyperpolarisability β with increasing electron accepting capability of the cationic borabenzene moiety. Unfortunately, the β values of the present cationic borabenzene complexes are rather small compared to other ferrocene containing donor-acceptor compounds. However, regarding the inertness of the complexes under study and the possibility to increase the SHG effect more than a factor of two when changing the pentamethylated cyclopentadienyl li-

gand with a simple cyclopentadienyl ligand on the acceptor site [2s], and “vice versa” on the donor site [21] it would be worthwhile to synthesize and study corresponding dinuclear borabenzene complexes.

Experimental Section

Manipulations were carried out under a dry nitrogen atmosphere using standard Schlenk technique. Solvents were saturated with nitrogen, diethyl ether (Et₂O), tetrahydrofuran (THF), *n*-hexane and toluene were freshly distilled from the appropriate alkali metal or metal alloy. Dichloromethane (CH₂Cl₂), acetonitril (MeCN) and nitromethane (MeNO₂) were dried over calcium hydride. NMR: Varian Gemini 200 BB; Bruker AM 360; measured at 295 K rel. TMS. UV-vis: Perkin-Elmer Model 554. IR: KBr pills, FT-IR, Perkin-Elmer Model 325. MS: Finnigan MAT 311 A. Elemental analyses: CHN-O-Rapid, Fa. Heraeus (Zentrale Elementanalytik, Fachbereich Chemie, Universität Hamburg). Trimethylphosphane borabenzene [6a], ethynylferrocene [2d], di[chloro- μ -chloro(η^6 -benzene)ruthenium(II)] [22], di[chloro- μ -chloro(η^5 -pentamethylcyclopentadienyl)rhodium(III)] [23], and di[chloro- μ -chloro(η^5 -pentamethylcyclopentadienyl)iridium(III)] [24] were synthesized according to the literature.

Lithium [1-ferrocenyl-2-(boratabenzene)ethyne] (2)

A solution of trimethylphosphane borabenzene (1) (455 mg, 2.86 mmol) and lithium ferrocenylacetylide (658 mg, 3.05 mmol) in THF (30 mL) was stirred for 30 min at room temperature and an additional 1 h under reflux. The reaction mixture was allowed to cool to room temperature and was evaporated to dryness. The sticky oily residue was stirred with a portion of benzene (20 mL) to dissolve residual PMe₃ and the obtained suspension was again evaporated to dryness. This procedure was repeated until the residue became an ochre coloured solid material, which was filtered and washed with *n*-hexane and dried *in vacuo*. Yield: 695 mg (83 %) of 2.

¹H NMR ([D₈]THF rel. TMS): δ = 4.02 (t, *J* = 1.8 Hz, 2 H, C₅H₄), 4.12 (s, 5 H, C₅H₅), 4.24 (t, *J* = 1.8 Hz, 2 H, C₅H₄), 6.09 (t, *J* = 7.3 Hz, 1 H, H-4), 6.51 (d, *J* = 9.9 Hz, 2 H, H-2,6), 7.07 (dd, *J* = 9.9, 7.3 Hz, H-3,5).

Thallium [1-ferrocenyl-2-(boratabenzene)ethyne] (3)

The lithium salt 2 (1.08 g, 3.7 mmol) and thallium chloride (1.34 g, 5.6 mmol) were stirred in MeCN (40 mL) for 1 h at room temperature and overnight at 50 °C. The reaction mixture was evaporated to dryness, the red solid material was dissolved in a small amount of pyridine and filtered. The filtrate was evaporated to dryness. The dry residue was suspended in MeCN whereupon an ochre coloured precipitate was formed. The precipitate was filtered off, washed with Et₂O and dried *in vacuo*. Yield: 190 mg (10.5 %) of 3.

Anal. calc. for (C₁₇H₁₄BFcTl)1/2(C₅H₅N), 528.9: C 44.28, H 3.14, N 1.32; found C 44.0, H 3.43, N 0.91 %.

¹H NMR ([D₆]DMSO, rel. TMS): δ = 4.12 (t, *J* = 1.8 Hz, 2 H, C₅H₄), 4.16 (s, 5 H, C₅H₅), 4.32 (t, *J* = 1.8 Hz, 2 H, C₅H₄), 6.02 (t, *J* = 7.1 Hz, 1 H, H-4), 6.30 (d, *J* = 9.8 Hz, 2 H, H-2,6), 6.89 (dd, *J* = 9.8, 7.1 Hz, 2 H, H-3,5); 7.39 (m, 1 H, C₅H₅N), 7.78 (m, 0.5 H, C₅H₅N), 8.56 (d, *J* = 4.1 Hz, 1 H, C₅H₅N); ¹³C NMR ([D₆] DMSO, rel. TMS): δ = 67.3 (C₅H₄), 69.4 (C₅H₅), 69.9 (C₅H₄), 111.2, 123.9 (C₅H₅N); 128.3, 130 (br, C-2,6), 131.7 (C-3,5), 136.2 (C₅H₅N), 149.6 (C₅H₅N); IR (KBr): $\tilde{\nu}$ = 3119, 3016, 2159 (ν_{C=C}), 1521, 1412, 1102, 1091, 744 cm⁻¹.

General Procedure of the Synthesis of [(η^5 -C₅H₅)Fe(μ -(η^5 -C₅H₄)C₂(η^6 -BC₅H₅)ML)]PF₆ (ML = Ru(η^6 -C₆H₆) (4aPF₆), Rh(η^5 -C₅Me₅) (4bPF₆), Ir(η^5 -C₅Me₅) (4cPF₆))

For the synthesis of 4aPF₆ – 4cPF₆ the thallium salt 3 was not isolated. The reaction mixture obtained from the synthesis of 3 (*vide supra*) was directly treated with an appropriate amount of the corresponding ruthenium, rhodium and iridium halide (*vide infra*). After stirring for 2 h at room temperature, 5 h at 40 – 50 °C and finally overnight at room temperature again, the reaction mixture was filtered and the filtrate evaporated to dryness. The residue was redissolved in water and filtered. Solid NH₄PF₆ was added to the water solution whereupon an orange coloured solid material was formed. The product was several times recrystallised from dichloromethane/diethyl ether.

4aPF₆: Used quantities: 2 (279 mg, 0.96 mmol), TiCl₄ (345 mg, 1.44 mmol), MeCN (40 mL) and [Ru(η^6 -C₆H₆)Cl(μ -Cl)]₂ (226 mg, 0.45 mmol). Yield: 315 mg (54 %) orange-coloured solid material.

Anal. calc. for C₂₃H₂₀BFcRuPF₆ (609.1): C 45.35, H 3.31; found: C 44.83, H 3.37 %.

¹H NMR ([D₆]acetone, rel. TMS): δ = 4.25 (s, 5 H, C₅H₅), 4.32 (br s, 2 H, C₅H₄), 4.50 (br s, 2 H, C₅H₄), 5.39 (m, 2 H, BC₅H₅), 6.39 (m, 3 H, BC₅H₅), 6.60 (s, 6 H, C₆H₆); ¹³C NMR ([D₆]acetone, rel. TMS): δ = 69.9 (C₅H₄), 70.9 (C₅H₅), 72.6 (C₅H₄), 86.4 (C-4), 90.5 (C₆H₆), 99.0 (C-3,5); IR (KBr): $\tilde{\nu}$ = 3097, 2166 (ν_{C=C}), 1485, 1444, 1406, 1106, 838 (ν_{P-F}), 558 cm⁻¹; UV-vis (CH₂Cl₂): λ_{max} (ϵ) = 288 (11120), 370 (sh), 446 (970) nm (M⁻¹cm⁻¹); (MeCN): λ_{max} (ϵ) = 288 (8080), 355 (sh), 440 (sh) nm (M⁻¹cm⁻¹); MS (FAB): *m/z* (%) = 465 (100) M⁺ + 1-PF₆;

4bPF₆: Used quantities: 2 (700 mg, 2.4 mmol), TiCl₄ (863 mg, 3.6 mmol), MeCN (60 mL), [RhCl(μ -Cl)(η^5 -C₅Me₅)]₂ (750 mg, 1.2 mmol). Yield: 1.06 g (67 %) red needles.

Anal. calc. for: C₂₇H₂₉BFcRhPF₆ (668.1): C 48.54, H 4.38; found C 47.99, H 4.33 %.

¹H NMR ([D₆]acetone, rel. TMS): δ = 2.26 (s, 15 H, C₅Me₅), 4.28 (s, 5 H, C₅H₅), 4.33 (t, *J* = 1.8 Hz, 2 H, C₅H₄), 4.55 (t, *J* = 1.8 Hz, 2 H, C₅H₄), 5.62 (d, *J* = 8.6 Hz, 2 H, H-2,6), 6.52 (t, *J* = 6.0 Hz, 1 H, H-4), 6.68 (dd, *J* = 8.6, 6.0 Hz, 2 H, H-3,5); (CD₂Cl₂, rel. TMS): δ = 2.12 (s, 15 H, C₅Me₅), 4.26 (s, 5 H, C₅H₅), 4.30 (t, *J* = 1.8 Hz, 2 H, C₅H₄), 4.52 (t, *J* = 1.8 Hz, 2 H, C₅H₄), 5.44 (d, *J* = 8.5 Hz, 2 H, H-2,6), 6.26 (t, *J* = 6.0 Hz, 1 H, H-4), 6.39 (dd, *J* = 8.5, 6.0 Hz, 2 H, H-3,5); IR (KBr): $\tilde{\nu}$ = 3092, 2156 (ν_{C=C}), 1490, 1403, 1105, 1026, 837 (ν_{P-F}), 558 cm⁻¹; UV-vis (CH₂Cl₂): λ_{max} (ϵ) = 293 (12200), 335 (7070), 456 (1330) nm (M⁻¹cm⁻¹), (MeCN): λ_{max} (ϵ) = 290 (12480), 331 (5810), 450 (sh) nm (M⁻¹cm⁻¹);

4cPF₆: Used quantities: 2 (510 mg, 1.8 mmol), TiCl₄ (648 mg, 2.7 mmol), MeCN (30 mL), [IrCl(μ -Cl)(η^5 -C₅Me₅)]₂ (710 mg, 0.89 mmol). Yield: 909 mg (67 %).

Anal. calc. for: C₂₇H₂₉BFcIrPF₆ (757.4): C 42.82, H 3.86; found C 42.37, H 4.16.

¹H NMR ([D₆]acetone, rel. TMS): δ = 2.36 (s, 15 H, C₅Me₅), 4.26 (s, 5 H, C₅H₅), 4.31 (t, *J* = 1.9 Hz, 2 H, C₅H₄), 4.52 (t, *J* = 1.9 Hz, 2 H, C₅H₄), 5.64 (m, 2 H, H-2,6), 6.65 (m, 3 H, H-3,5, H-4); (CD₂Cl₂, rel. TMS): δ = 2.23 (s, 15 H, C₅Me₅), 4.25 (s, 5 H, C₅H₅), 4.29 (t, *J* = 1.8 Hz, 2 H, C₅H₄), 4.49 (t, *J* = 1.8 Hz, 2 H, C₅H₄), 5.44 (d, *J* = 8.8 Hz, 2 H, H-2,6), 6.32 (m, 1 H, H-4), 6.36 (m, 2 H, H-3,5); ¹³C NMR ([D₆]acetone, rel. TMS): δ = 9.9 (C₅Me₅), 69.8 (C₅H₄), 70.7 (C₅H₅), 72.4 (C₅H₄), 87.6 (C-4), 99.3 (C₅Me₅), 100.8 (C-3,5); (CD₂Cl₂, rel. TMS): δ = 10.2 (C₅Me₅), 69.6 (C₅H₄), 70.4 (C₅H₅), 72.3 (C₅H₄), 86.4 (C-4), 92 (br, C-2,6), 98.7 (C₅Me₅), 99.9 (C-3,5); IR (KBr): $\tilde{\nu}$ = 3094, 2160 (ν_{C=C}), 1470, 1400, 1107, 1034, 837 (ν_{P-F}), 558 cm⁻¹; UV-vis (CH₂Cl₂): λ_{max} (ϵ) = 292 (18860), 360 (sh), 442 (980) nm (M⁻¹cm⁻¹); (MeCN): λ_{max} (ϵ) = 288 (12780), 350 (sh), 442 (480), nm (M⁻¹cm⁻¹);

4aBPh₄: 4aPF₆ (110 mg, 0.18 mmol) was dissolved in a minimum amount of CH₂Cl₂. An equimolar solution of Na[BPh₄] (62 mg, 0.18 mmol) in MeOH was added. The precipitation was filtered and recrystallised from MeCN/EtOH.

Anal. calcd. for (C₄₇H₄₀B₂FeRu) (783.4): C 72.06, H 5.15; found C 71.86, H 5.20 %.

Cyclic Voltammetry

Measurements were performed in CH₂Cl₂ with 0.4 M [N^{(t}Bu)₄]PF₆ as supporting electrolyte. An Amel 5000 system was used with a Pt wire as the working electrode and a Pt plate (0.6 cm²) as the auxiliary electrode. The potentials were measured against Ag/AgCl and are referenced against E_{1/2}([Fe(C₅H₅)₂]/[Fe(C₅H₅)₂]⁺) = 0 V.

X-ray Structure Determination

Crystals suitable for X-ray structure determination were obtained by gasphase diffusion of Et₂O into a concentrated solution of **4aBPh**₄ in MeCN and by diffusion of an Et₂O layer into a concentrated solution of **4bPF**₆ in CH₂Cl₂.

Single crystal X-ray diffraction studies of compound **4aBPh**₄ were performed on a Hilger & Watts four circle diffractometer with monochromated Mo-K_α radiation at 20 °C. For compound **4bPF**₆ a Bruker axis SMART CCD system was used (temperature -120 °C; Mo-K_α radiation). Both structures were solved by direct methods [25] and refined by SHELXTL [26, 27]. The crystal data and the conditions for data collection and refinement are summarized in Table 1. All atoms (except hydrogen) were refined using anisotropic thermal parameters. The hydrogen atoms were placed geometrically and refined using a riding model with isotropic thermal parameters equal to 1.2 (CH) or 1.5 (CH₃) U_{eq} of the carbon atoms to which they are attached.

The crystallographic data for the structures reported in this paper have been deposited at the Cambridge Data Centre as supplementary publication no. CCDC-207476 (**4aBPh**₄), and CCDC-207477 (**4bPF**₆). These data can be obtained free of charge at www.ccdc.cam.ac.uk/conts/retrieving.html or from the Cambridge Crystallographic Centre, 12 Union Road, Cambridge CB2 1EZ, UK [fax: (internat.) + 44-1223/336-033; e-mail: deposit@ccdc.cam.ac.uk].

HRS measurements of the first hyperpolarisabilities

Hyper-Rayleigh scattering measurements were performed with a pulsed Nd:YAG laser at a wavelength of λ = 1064 nm. For the experimental setup see ref. [17b]. Solutions of the complexes in MeNO₂ with concentrations in the range of 10⁻⁴ to 10⁻⁶ M were used with *p*-nitroaniline as a reference [β(MeNO₂) = 34.6 × 10⁻³⁰ esu] [28]. Fluorescence checks were made by replacing the interference filter in front of the photomultiplier tube with filters that have transmittances at 400, 450, 500, 560, 600, and 700 nm [19].

Acknowledgments: This work was supported by the Deutsche Forschungsgemeinschaft (DFG, HE 1309/3), by the European Community (COST D4/003/94, TMR FMRX-CT98-0166) and by the Fonds der Chemischen Industrie. We thank the DEGUSSA AG for a donation of RuCl₃ and Sartorius GmbH for a donation of micro-filters.

References

- [1] a) D. J. Williams, *Angew. Chem.* **1984**, *96*, 637–651; *Angew. Chem. Int. Ed. Engl.* **1984**, *23*, 690–703; b) R. W. Boyd in: *Nonlinear Optics*, Academic Press, Inc, **1992**; c) G. H. Wagnier

- in: *Linear and Nonlinear Optical Properties of Molecules*, VCH, Weinheim, **1993**; d) P. N. Prasad, D. J. Williams in: *Nonlinear Optical Effects In Molecules & Polymers*, Wiley & Sons, New York, **1991**; e) H. S. Nalwa, *Appl. Organomet. Chem.* **1991**, *5*, 349–377; f) T. J. Marks, M. A. Ratner, *Angew. Chem.* **1995**, *107*, 167–187; *Angew. Chem. Int. Ed. Engl.* **1995**, *34*, 155–174; g) N. J. Long, *Angew. Chem.* **1995**, *107*, 37–56; *Angew. Chem. Int. Ed. Engl.* **1995**, *34*, 21–38; i) H. S. Nalwa, S. Miyata (ed.) in: *Nonlinear Optics of Organic Molecules and Polymers*, CRC Press, New York, **1997**; j) K. Meerholz, *Angew. Chem.* **1997**, *109*, 981–985; *Angew. Chem. Int. Ed. Engl.* **1997**, *36*, 945–949; k) T. Verbiest, S. Houbrechts, M. Kauranen, K. Clays, A. Persoons, *J. Mater. Chem.* **1997**, *7*, 2175–2189; l) I. R. Whittall, A. M. McDonagh, M. G. Humphrey, M. Samoc, *Adv. Organomet. Chem.* **1998**, *42*, 291–362; m) B. J. Coe, *Chem. Eur. J.* **1999**, *5*, 2464–2471; n) M. Kauranen, T. Verbiest, A. Persoons, *J. Nonl. Opt. Phys. Mater.* **1999**, *2*, 171–189. [2] a) W. M. Laidlaw, R. G. Denning, T. Verbiest, E. Chauchard, A. Persoons, *Nature*, **1993**, *363*, 58–59; W. M. Laidlaw, R. G. Denning, T. Verbiest, E. Chauchard, A. Persoons, *Proc. SPIE, Int. Soc. Opt. Eng.* **1994**, *2143*, 14–19; B. J. Coe, J. P. Essex-Lopresti, J. A. Harris, S. Houbrechts, A. Persoons, *Chem. Commun.* **1997**, 1645–1646; b) S. Houbrechts, K. Clays, A. Persoons, V. Cadierno, M. P. Gamasa, J. Gimeno, *Organometallics* **1996**, *15*, 5266–5268; V. Cadierno, S. Conejero, M. P. Gamasa, J. Gimeno, I. Asselberghs, S. Houbrechts, K. Clays, A. Persoons, J. Borge, S. Garcia-Granda, *Organometallics* **1999**, *18*, 582–597; M.H. Garcia, S. Royer, M.P. Robalo, A. R. Dias, J.-P. Tranchier, R. Chavignon, D. Prim, A. Auffrant, F. Rose-Munch, E. Rose, J. Vaisserman, A. Persoons, I. Asselberghs, *Eur. J. Inorg. Chem.* **2002**, accepted; c) B. J. Coe, J.-D. Foulon, T. A. Hamor, C. J. Jones, J. A. McCleverty, D. Bloor, G. H. Cross, T. L. Axon, *J. Chem. Soc. Dalton Trans.* **1994**, 3427–3439; d) U. Behrens, H. Brussaard, U. Hagenau, J. Heck, E. Hendrickx, J. Körnich, J. G. M. van der Linden, A. Persoons, A. L. Spek, N. Veldman, B. Voss, H. Wong, *Chem. Eur. J.* **1996**, *2*, 98–103; e) E. Hendrickx, A. Persoons, S. Samson, G. R. Stephenson, *J. Organomet. Chem.* **1997**, *542*, 295–297; f) M. C. B. Colbert, J. Lewis, N. J. Long, P. R. Raithby, A. J. P. White, D. J. Williams, *J. Chem. Soc., Dalton Trans.* **1997**, 99–104; g) J. Mata, S. Uriel, E. Peris, R. Llusar, S. Houbrechts, A. Persoons, *J. Organomet. Chem.* **1998**, *562*, 197–202; h) O. Briel, A. Fehn, K. Polborn, W. Beck, *Polyhedron*, **1998**, *18*, 225–242; i) I. S. Lee, S. S. Lee, Y. K. Chung, D. Kim, N. W. Song, *Inorg. Chim. Acta* **1998**, *279*, 243–248; j) J. Heck, S. Dabek, T. Meyer-Friedrichsen, H. Wong, *Coord. Chem. Rev.* **1999**, *190–192*, 1217–1254; k) O. Briel, K. Sünkel, I. Krossing, H. Nöth, E. Schmäzlin, K. Meerholz, C. Bräuchle, W. Beck, *Eur. J. Inorg. Chem.* **1999**, 483–490; l) K. N. Jayaprakash, P. C. Ray, I. Matsuoka, M. M. Bhadhbade, V. G. Puranik, P. K. Das, H. Nishihara, A. Sarkar, *Organometallics* **1999**, *18*, 3851–3858; m) H. Le Bozec, T. Renouard, *Eur. J. Inorg. Chem.* **2000**, 229–239; n) T. Farrell, T. Meyer-Friedrichsen, M. Malessa, D. Haase, W. Saak, I. Asselberghs, K. Wostyn, K. Clays, A. Persoons, J. Heck, A. R. Manning, *J. Chem. Soc., Dalton Trans.* **2001**, 29–36; o) J. A. Mata, E. Peris, I. Asselberghs, R. von Boxel, A. Persoons, *New J. Chem.* **2001**, 1043–1046; p) T. Farrell, A. R. Manning, T. C. Murphy, T. Meyer-Friedrichsen, J. Heck, I. Asselberghs, A. Persoons, *Eur. J. Inorg. Chem.* **2001**, 2365–2375; q) M. Malaun, R. Kowallick, A. M. McDonagh, M. Marcaccio, R. L. Paul, I. Asselberghs, K. Clays, A. Persoons, B. Bildstein, C. Fiorini, J.-M. Nunzi, M. D. Ward, J. A. McCleverty, *J. Chem. Soc.*

- Dalton Trans.* **2001**, 3025–3038; r) T. Farrell, A. R. Manning, G. Mitchell, J. Heck, T. Meyer-Friedrichsen, M. Malessa, C. Wittenburg, M. H. Prosenc, D. Cunningham, P. McArdle, *Eur. J. Inorg. Chem.* **2002**, 1677–1686; s) T. Meyer-Friedrichsen, C. Mecker, M. H. Prosenc, J. Heck, *Eur. J. Inorg. Chem.* **2002**, 239–248; t) T. Meyer-Friedrichsen, H. Wong, M. H. Prosenc, J. Heck, *Eur. J. Inorg. Chem.* **2003**, 936–946.
- [3] U. Hagenau, J. Heck, E. Hendrickx, A. Persoons, T. Schuld, H. Wong, *Inorg. Chem.* **1996**, *35*, 7863–7866.
- [4] G. E. Herberich, W. Koch, H. Lueken, *J. Organomet. Chem.* **1978**, *160*, 17–23.
- [5] S. Qiao, D. A. Hoic, G. C. Fu, *J. Am. Chem. Soc.* **1996**, *118*, 6329–6330.
- [6] a) A. J. Ashe III, J. W. Kampf, C. Müller, M. Schneider, *Organometallics* **1996**, *15*, 387–393; b) D. A. Hoic, J. R. Wolf, W. M. Davis, G. C. Fu, *Organometallics* **1996**, *15*, 1315–1318.
- [7] a) G. E. Herberich, H. J. Becker, C. Engelke, *J. Organomet. Chem.* **1978**, *153*, 265–270; b) G. E. Herberich, H. J. Becker, K. Carsten, C. Engelke, W. Koch, *Chem. Ber.* **1976**, *109*, 2382–2388; c) G. E. Herberich, C. Engelke, W. Pahlmann, *Chem. Ber.* **1979**, *112*, 607–624.
- [8] a) G. E. Herberich, W. Klein, T. P. Spaniol, *Organometallics* **1993**, *12*, 2660–2667; b) G. E. Herberich, B. Schmidt, U. Englert, T. Wagner, *Organometallics* **1993**, *12*, 2891–2893; c) M. C. Amendola, K. E. Stockman, D. A. Hoic, W. M. Davis, G. C. Fu, *Angew. Chem.* **1997**, *109*, 278–281; *Angew. Chem. Int. Ed. Engl.*, **1997**, *36*, 267–269; d) G. E. Herberich, W. Boveleth, B. Hessner, W. Koch, E. Raabe, D. Schmitz, *J. Organomet. Chem.* **1984**, *265*, 225–235.
- [9] G. E. Herberich, U. Englert, D. Pubanz, *J. Organomet. Chem.* **1993**, *459*, 1–9; A. J. Ashe, III, X. Fang, J. W. Kampf, *Organometallics* **1999**, *18*, 466–473.
- [10] A. E. Stieglmann, E. Graham, K. J. Perry, L. R. Khundkar, L.-T. Cheng, J. W. Perry, *J. Am. Chem. Soc.* **1991**, *113*, 7658–7666.
- [11] C. Dehu, F. Meyers, J. L. Brédas, *J. Am. Chem. Soc.* **1993**, *115*, 6198–6206.
- [12] H. Schulz, G. Gabbert, H. Pritzkow, W. Siebert, *Chem. Ber.* **1993**, *126*, 1593–1595.
- [13] V. Bachler, N. Metzler-Nolte, *Eur. J. Inorg. Chem.* **1998**, 733–744.
- [14] G. E. Herberich, U. Englert, B. Ganter, C. Lamertz, *Organometallics* **1996**, *15*, 5236–5241.
- [15] a) An explanation for the reoxidation step at -0.6 V vs [FcH]/[FcH]⁺ may be the oxidation of a dimerisation product which could be formed upon the reduction as it is found for other 19 VE sandwich complexes. [15b] The redox chemistry of **4b**PF₆ will be subject of a more detailed electrochemical analysis. b) D. Astruc in: *Electron Transfer and Radical Process in Transition-Metal Chemistry*, VCH Publishers, Weinheim, Germany, **1995**, p. 337 ff.
- [16] P. Suppan, N. Ghoneim, in *Solvatochromism*, Paston Press, LTD, Norfolk, **1997**; N. Matage, T. Kubota, *Molecular Interactions and Electronic Spectra*; Marcel Dekker; New York, **1970**, chapter 8.
- [17] a) R. W. Terhune, P. D. Maker, C. M. Savage, *Phys. Rev. Lett.* **1962**, *8*, 404–406; b) K. Clays, A. Persoons, *Rev. Sci. Instrum.* **1992**, *63*, 3285–3289.
- [18] a) K. Clays, E. Hendrickx, T. Verbiest, A. Persoons, *Adv. Mater.* **1998**, *10*, 643–655; G. Olbrechts, T. Munters, K. Clays, A. Persoons, O.-K. Kim, L.-S. Choi, *Opt. Mat.* **1999**, *12*, 221; b) J.J. Wolff, R. Wortmann, *Adv. Phys. Org. Chem.* **1999**, *32*, 121–217; c) S. Stadler, G. Bourhill, C. Bräuchle, *J. Phys. Chem.* **1996**, *100*, 6927–6934; d) S. Stadler, R. Dietrich, G. Bourhill, C. Bräuchle, *Optics Letts.* **1996**, *21*, 251–253; e) M. A. Pauley, C. H. Wang, *Rev. Sci. Instrum.* **1999**, *70*, 1277–1284; f) N. W. Song, T.-I. Kang, S. C. Jeung, S.-J. Joan, B. R. Cho, D. Kim, *Chem. Phys. Lett.* **1996**, *261*, 307–312; g) O. K. Song, J. N. Woodford, C. H. Wang, *J. Phys. Chem. A.* **1997**, *101*, 3222–3226.
- [19] H. Wong, T. Meyer-Friedrichsen, T. Farrell, Ch. Mecker, J. Heck, *Eur. J. Inorg. Chem.* **2000**, 631–646;
- [20] The failure of the β value for **4a**PF₆ may be a result of the relatively high threshold for the determination of the β values by means of our HRS set-up. Our experience demonstrate a reliable determination of β -values beyond 30×10^{-30} esu.
- [21] T. Meyer-Friedrichsen, M. H. Prosenc, J. Heck, manuscript in preparation.
- [22] T. A. Stephenson, D. A. Tocher, *Organomet. Synth.* **1986**, *3*, 99–103.
- [23] J. W. Kang, K. Moseley, P. M. Maitlis, *J. Am. Chem. Soc.* **1969**, *91*, 5970–5977.
- [24] G. Fairhurst, C. White, *J. Chem. Soc., Dalton Trans.* **1979**, 1524–1530.
- [25] G. M. Sheldrick, SHELXS-86 program for crystal structure determination, University of Göttingen, Germany, **1986**.
- [26] G. M. Sheldrick, SHELXL-93 program for crystal structure refinement, University of Göttingen, Germany, **1993**.
- [27] G. M. Sheldrick, SHELXL-97, program for crystal structure refinement, University of Göttingen, Germany, **1997**.
- [28] T. Verbiest, K. Clays, S. Samyn, J. Wolff, D. Reinhoudt, A. Persoons, *J. Am. Chem. Soc.* **1994**, *116*, 9320–9323.